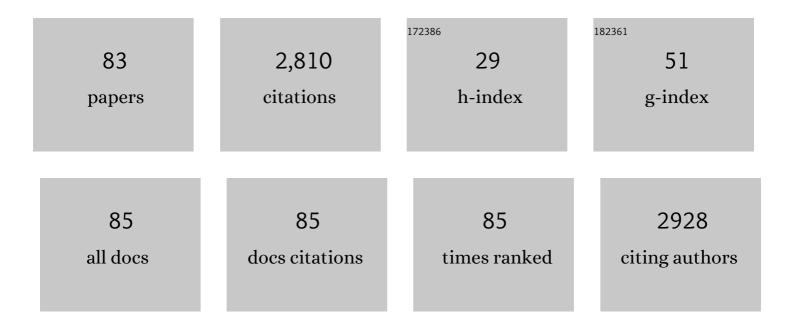
## Sheng-Run Zheng

List of Publications by Year in descending order

Source: https://exaly.com/author-pdf/6736169/publications.pdf Version: 2024-02-01



#	Article	IF	CITATIONS
1	Tunable electrical conductivity in oriented thin films of tetrathiafulvalene-based covalent organic framework. Chemical Science, 2014, 5, 4693-4700.	3.7	295
2	Stable Hydrazone-Linked Covalent Organic Frameworks Containing O,N,Oâ€2-Chelating Sites for Fe(III) Detection in Water. ACS Applied Materials & Interfaces, 2019, 11, 12830-12837.	4.0	152
3	The construction of amorphous metal-organic cage-based solid for rapid dye adsorption and time-dependent dye separation from water. Chemical Engineering Journal, 2019, 357, 129-139.	6.6	129
4	2-Fold Interpenetrating Bifunctional Cd-Metal–Organic Frameworks: Highly Selective Adsorption for CO <sub>2</sub> and Sensitive Luminescent Sensing of Nitro Aromatic 2,4,6-Trinitrophenol. ACS Applied Materials & Interfaces, 2017, 9, 4701-4708.	4.0	113
5	Regulation of the surface area and surface charge property of MOFs by multivariate strategy: Synthesis, characterization, selective dye adsorption and separation. Microporous and Mesoporous Materials, 2018, 272, 101-108.	2.2	112
6	Construction of a hydrazone-linked chiral covalent organic framework–silica composite as the stationary phase for high performance liquid chromatography. Journal of Chromatography A, 2017, 1519, 100-109.	1.8	110
7	Hydrolytically Stable Nanotubular Cationic Metal–Organic Framework for Rapid and Efficient Removal of Toxic Oxo-Anions and Dyes from Water. Inorganic Chemistry, 2019, 58, 2899-2909.	1.9	106
8	Metal-Directed Assembly of Coordination Polymers with a Multifunctional Semirigid Ligand Containing Pyridyl and Benzimidazolyl Donor Groups. Crystal Growth and Design, 2009, 9, 2341-2353.	1.4	92
9	Construction of Metal-Imidazole-Based Dicarboxylate Networks with Topological Diversity: Thermal Stability, Gas Adsorption, and Fluorescent Emission Properties. Crystal Growth and Design, 2012, 12, 2178-2186.	1.4	87
10	Assembly of CdI2-type coordination networks from triangular ligand and octahedral metal center: topological analysis and potential framework porosity. Chemical Communications, 2008, , 356-358.	2.2	78
11	An Anionic Nanotubular Metal–Organic Framework for High-Capacity Dye Adsorption and Dye Degradation in Darkness. Inorganic Chemistry, 2019, 58, 13979-13987.	1.9	75
12	The construction of coordination networks based on imidazole-based dicarboxylate ligand containing hydroxymethyl group. CrystEngComm, 2011, 13, 883-888.	1.3	68
13	A Series of New Three-Dimensional d–f Heterometallic Coordination Polymers with Rare 10-Connected <b>bct</b> Net Topology Based on Planar Hexanuclear Heterometallic Second Building Units. Crystal Growth and Design, 2012, 12, 5737-5745.	1.4	67
14	Two Types of New Three-Dimensional d–f Heterometallic Coordination Polymers Based on 2-(Pyridin-3-yl)-1 <i>H</i> -Imidazole-4,5-Dicarboxylate and Oxalate Ligands: Syntheses, Structures, Luminescence, and Magnetic Properties. Crystal Growth and Design, 2012, 12, 4441-4449.	1.4	63
15	Construction of Ba(II) Coordination Polymers Based on Imidazole-Based Dicarboxylate Ligands: Structural Diversity Tuned by Alcohol Solvents. Crystal Growth and Design, 2012, 12, 3575-3582.	1.4	59
16	Rationally Designed 2D Covalent Organic Framework with a Brick-Wall Topology. ACS Macro Letters, 2016, 5, 1348-1352.	2.3	59
17	An unusual 3D coordination polymer assembled through parallel interpenetrating and polycatenating of (6,3) nets. CrystEngComm, 2009, 11, 680.	1.3	58
18	Assembly of Chiral/Achiral Coordination Polymers Based on 2-(Pyridine-3-yl)-1H-4,5-imidazoledicarboxylic Acid: Chirality Transfer between Chiral Two-Dimensional Networks Containing Helical Chains. Crystal Growth and Design, 2012, 12, 2355-2361.	1.4	57

SHENG-RUN ZHENG

#	Article	IF	CITATIONS
19	A hydrolytically stable cage-based metal–organic framework containing two types of building blocks for the adsorption of iodine and dyes. Inorganic Chemistry Frontiers, 2021, 8, 1083-1092.	3.0	55
20	Dimension Increase via Hydrogen Bonding and Weak Coordination Interactions from Simple Complexes of 2-(Pyridyl)benzimidazole Ligands. Crystal Growth and Design, 2007, 7, 2481-2490.	1.4	48
21	Construction of Ag(I)–Ln(III) Heterometallic Coordination Polymers Based on Binuclear Ag <sub>2</sub> (DSPT) <sub>2</sub> (H <sub>2</sub> DSPT = 4′-(2,4-Disulfophenyl)-2,2′:6′2″-terpyri Rings and Ln(III) Dimeric Molecular Building Blocks. Crystal Growth and Design, 2013, 13, 4428-4434.	dinæ)	43
22	Reversible Interlayer Sliding and Conductivity Changes in Adaptive Tetrathiafulvalene-Based Covalent Organic Frameworks. ACS Applied Materials & Interfaces, 2020, 12, 19054-19061.	4.0	40
23	Construction of terpyridine–Ln(iii) coordination polymers: structural diversity, visible and NIR luminescence properties and response to nerve-agent mimics. CrystEngComm, 2014, 16, 2898.	1.3	39
24	An unprecedented (3,4,14)-connected 3D metal–organic framework based on planar octanuclear lead(ii) clusters as a secondary building unit. CrystEngComm, 2012, 14, 1193-1196.	1.3	36
25	Anion-dependent assembly and solvent-mediated structural transformations of three Cd(ii) coordination polymers based on 1H-imidazole-4-carboxylic acid. CrystEngComm, 2012, 14, 2308.	1.3	36
26	Assembly of Cd( <scp>ii</scp> ) coordination polymers: structural variation, supramolecular isomers, and temperature/anion-induced solvent-mediated structural transformations. CrystEngComm, 2015, 17, 947-959.	1.3	36
27	Construction of four 3d-4d/4d complexes based on salen-type schiff base ligands. CrystEngComm, 2011, 13, 6911.	1.3	34
28	Facile and Site-Selective Synthesis of an Amine-Functionalized Covalent Organic Framework. ACS Macro Letters, 2021, 10, 1590-1596.	2.3	32
29	Synthesis, crystal structures and properties of Ln(iii)–Cu(i)–Na(i) and Ln(iii)–Ag(i) heterometallic coordination polymers. CrystEngComm, 2011, 13, 3910.	1.3	29
30	Construction of luminescent three-dimensional Ln(iii)–Zn(ii) heterometallic coordination polymers based on 2-pyridyl imidazole dicarboxylate. CrystEngComm, 2012, 14, 8236.	1.3	29
31	Cationic Amorphous Metal–Organic Cage-Based Materials for the Removal of Oxo-Anions from Water. ACS Applied Nano Materials, 2019, 2, 5824-5832.	2.4	28
32	A new hydrazone-linked covalent organic framework for Fe( <scp>iii</scp> ) detection by fluorescence and QCM technologies. CrystEngComm, 2021, 23, 3594-3601.	1.3	28
33	The construction of Cu(i)/Cu(ii) coordination polymers based on pyrazine–carboxylate: Structural diversity tuned by in situ hydrolysis reaction. CrystEngComm, 2013, 15, 5359.	1.3	26
34	A Benzimidazole-Containing Covalent Organic Framework-Based QCM Sensor for Exceptional Detection of CEES. Crystal Growth and Design, 2019, 19, 3543-3550.	1.4	26
35	An unprecedented 2D covalent organic framework with an htb net topology. Chemical Communications, 2019, 55, 13454-13457.	2.2	26
36	Homochiral Cu(I) Coordination Polymers Based on a Double-Stranded Helical Building Block from Achiral Ligands: Symmetry-Breaking Crystallization, Photophysical and Photocatalytic Properties. Inorganic Chemistry, 2019, 58, 14660-14666.	1.9	25

#	Article	IF	CITATIONS
37	Anion- and temperature-dependent assembly, crystal structures and luminescence properties of six new Cd( <scp>ii</scp> ) coordination polymers based on 2,3,5,6-tetrakis(2-pyridyl)pyrazine. CrystEngComm, 2016, 18, 5164-5176.	1.3	24
38	Syntheses and conversions of dinuclear cadmium(ii) compounds containing N2O/N2O2 donor tridentate/tetradentate asymmetrical Schiff base ligands. CrystEngComm, 2010, 12, 4012.	1.3	23
39	Amorphous metal–organic frameworks obtained from a crystalline precursor for the capture of iodine with high capacities. Chemical Communications, 2022, 58, 5013-5016.	2.2	22
40	A recyclable bipyridine-containing covalent organic framework-based QCM sensor for detection of Hg(II) ion in aqueous solution. Journal of Solid State Chemistry, 2021, 302, 122421.	1.4	19
41	An unprecedented supramolecular network with channels filled by 1D coordination polymer chains: Cocrystallization of Ag(i)-4,4′-bipyridine and Ag(i)-benzimidazole complexes. CrystEngComm, 2011, 13, 6345.	1.3	17
42	Cu-MOF derived Cu–C nanocomposites towards high performance electrochemical supercapacitors. RSC Advances, 2020, 10, 4621-4629.	1.7	17
43	Construction of several new s-/p-block complexes containing binuclear metal–terpyridine building blocks: dependence of structural diversity on the number of coordinated water molecules. CrystEngComm, 2014, 16, 4029.	1.3	16
44	Construction of six new luminescent Ln( <scp>iii</scp> )–Zn( <scp>ii</scp> ) heterometallic coordination polymers based on heterometallic secondary building units. CrystEngComm, 2016, 18, 8672-8682.	1.3	16
45	A series of alkaline earth metal coordination polymers constructed from two newly designed imidazole-based dicarboxylate ligands containing pyridinylmethyl groups. CrystEngComm, 2017, 19, 3003-3016.	1.3	16
46	Two new three-dimensional metal–organic frameworks with 4-connected diamondoid and unusual (6,16)-connected net topologies based on planar tetranuclear squares as secondary building units. CrystEngComm, 2016, 18, 1174-1183.	1.3	15
47	Fabrication of a hydrazoneâ€linked covalent organic frameworkâ€bound capillary column for gas chromatography separation. Separation Science Plus, 2019, 2, 120-128.	0.3	14
48	Spontaneous resolution of a coordination polymer containing stereogenic five-coordinate Zn(ii) centers and achiral ligands with axially chiral conformation. CrystEngComm, 2012, 14, 6241.	1.3	13
49	A new QCM signal enhancement strategy based on streptavidin@metal-organic framework complex for miRNA detection. Analytica Chimica Acta, 2020, 1095, 212-218.	2.6	13
50	Transformation of a Hydrazone-Linked Covalent Organic Framework into a Highly Stable Hydrazide-Linked One. ACS Applied Polymer Materials, 2022, 4, 4624-4631.	2.0	13
51	Syntheses, structures, and properties of nine d10or p-block coordination polymers based on a ligand containing both terpyridyl and sulfo groups. CrystEngComm, 2015, 17, 5538-5550.	1.3	12
52	A Mn( <scp>ii</scp> )–MOF with inherent missing metal-ion defects based on an imidazole-tetrazole tripodal ligand and its application in supercapacitors. Dalton Transactions, 2020, 49, 12150-12155.	1.6	11
53	Fabrication of cellulose derivative coated spherical covalent organic frameworks as chiral stationary phases for high-performance liquid chromatographic enantioseparation. Journal of Chromatography A, 2022, 1675, 463155.	1.8	11
54	Structures and luminescent properties of four compounds based on binuclear metal-terpyridine building blocks. Journal of Coordination Chemistry, 2016, 69, 966-975.	0.8	9

SHENG-RUN ZHENG

#	Article	IF	CITATIONS
55	Lanthanide contraction effect on the crystal structures of 2D lanthanide coordination polymers based on 2-(trifluoromethyl)-1H-imidazole-4,5-dicarboxylic acid. Structural Chemistry, 2017, 28, 577-586.	1.0	9
56	A hydrolytically stable hydrogen-bonded inorganic-organic network as a luminescence turn-on sensor for the detection of Bi3+ and Fe3+ cations in water. Polyhedron, 2021, 205, 115284.	1.0	9
57	trans-Diaquabis(1H-imidazole-4-carboxylato-κ2N3,O4)nickel(II). Acta Crystallographica Section E: Structure Reports Online, 2011, 67, m865-m865.	0.2	8
58	Construction of Four Coordination Polymers based on 2-[4-(Pyridine-4-yl)phenyl]-1 <i>H</i> -imidazole-4,5-dicarboxylic Acid. Zeitschrift Fur Anorganische Und Allgemeine Chemie, 2017, 643, 593-600.	0.6	8
59	Covalent Crossâ€Linking of Metalâ€Organic Cages: Formation of an Amorphous Cationic Porous Extended Framework for the Uptake of Oxoâ€Anions from Water. ChemPlusChem, 2021, 86, 709-715.	1.3	8
60	The construction of two lanthanide coordination polymers based on 5-hydroxyisophthalate and bipyridine. Journal of Coordination Chemistry, 2013, 66, 2659-2668.	0.8	7
61	Construction of coordination polymers based on a rigid tripodal nitrogen-containing heterotopic ligand that designed by mixed-donors strategy. Journal of Solid State Chemistry, 2018, 265, 64-71.	1.4	7
62	A Ni( <scp>ii</scp> ) metal–organic framework with helical channels for the capture of iodine <i>via</i> guest exchange induced amorphization. New Journal of Chemistry, 0, , .	1.4	7
63	Two Coordination Polymers Constructed from 5â€(4â€Pyridyl)â€1Hâ€tetrazole Ligands with Different Organic Carboxylates: Structure and Luminescence Properties. Zeitschrift Fur Anorganische Und Allgemeine Chemie, 2014, 640, 2057-2061.	0.6	6
64	Construction of four d <sup>10</sup> coordination polymers containing binuclear rings as building blocks from 4′-(2H-tetrazol-5-yl)biphenyl-4-carboxylic acid. Journal of Coordination Chemistry, 2016, 69, 976-984.	0.8	6
65	Construction of d <sup>10</sup> metal coordination polymers based on <i>in situ</i> formed 3,5-di(1 <i>H</i> -1,2,4-triazol-1-yl)benzoic acid from different precursors: influence of <i>in situ</i> hydrolysis reactions on assembly process. CrystEngComm, 2018, 20, 5531-5543.	1.3	6
66	The interaction of an amorphous metal–organic cage-based solid (aMOC) with miRNA/DNA and its application on a quartz crystal microbalance (QCM) sensor. Chemical Communications, 2020, 56, 591-594.	2.2	6
67	2,2′-(Iminodimethylene)bis(1H-benzimidazolium)(1+) chloride. Acta Crystallographica Section C: Crystal Structure Communications, 2005, 61, o642-o644.	0.4	4
68	Anion and pH-regulated assembly of three Cd(II) coordination polymers based on 3,5-di(1H-benzo[d]imidazol-1-yl)benzoate. Journal of Coordination Chemistry, 2017, 70, 135-144.	0.8	4
69	Assembly of a New 2D Heterometallic 3d–4f Coordination Polymer Bearing Planar Tetranuclear Square Building Blocks. Journal of Chemical Crystallography, 2019, 49, 21-28.	0.5	4
70	A new amplification strategy for a quartz crystal microbalance miRNA sensor based on selective interactions between a metal–organic framework and miRNA. New Journal of Chemistry, 2020, 44, 1684-1688.	1.4	4
71	Protein A-mesoporous silica composites for chromatographic purification of immunoglobulin G. New Journal of Chemistry, 2020, 44, 7884-7890.	1.4	4
72	Construction of Two 3D Main Group Coordination Polymers Based on 2â€(2â€Pyridyl)â€4,5â€imidazoleâ€dicarboxylic Acid: Structures and Luminescent Properties. Zeitschrift Fur Anorganische Und Allgemeine Chemie, 2015, 641, 2677-2682.	0.6	3

SHENG-RUN ZHENG

#	Article	IF	CITATIONS
73	Construction, crystal structures, and luminescence properties of three coordination polymers from the same precursor, 4-(1H-benzimidazol-1-yl)benzonitrile. Transition Metal Chemistry, 2015, 40, 699-706.	0.7	3
74	Synthesis of a New Cyclosporine-based Stationary Phase and Separation Behaviors toward Aromatic Positional Isomers by High-Performance Liquid Chromatography. Journal of Chromatographic Science, 2015, 53, 548-553.	0.7	3
75	Construction of a New 3D Zn(II) MOF with a mog Topology From 2-(Hydroxymethyl)-1H-imidazole-4,5-dicarboxylate. Journal of Chemical Crystallography, 2018, 48, 47-53.	0.5	3
76	Assembly of a miRNAâ€modified QCM sensor for miRNA recognition through response patterns. Journal of Molecular Recognition, 2019, 32, e2772.	1.1	3
77	A hydrolytically stable Zn(II) coordination polymer based on a new imidazolyl-pyrazolyl heterotopic ligand as a scavenger of MnO4â^' and a luminescent sensor for MnO4â^' and Cr2O72â^'. Inorganic Chemistry Communication, 2021, 130, 108720.	1.8	3
78	Synthesis, Crystal Structures and Thermal Stabilities of Lanthanide Coordination Polymers with 5-Nitroisophthalate. Journal of Inorganic and Organometallic Polymers and Materials, 2011, 21, 723-729.	1.9	2
79	Synthesis, crystal structure, supramolecular assembly, and thermal stability of two new lanthanide coordination polymers based on $\hat{l}_{\pm}$ -naphthoxyacetate. Structural Chemistry, 2011, 22, 943-949.	1.0	2
80	Crystal structure of [3-(1H-benzimidazol-2-yl)propanoato-κN3][3-(1H-benzimidazol-2-yl)propanoic acid-κN3]copper(I). Acta Crystallographica Section E: Crystallographic Communications, 2015, 71, m5-m6.	0.2	2
81	Covalent Crossâ€Linking of Metalâ€Organic Cages: Formation of an Amorphous Cationic Porous Extended Framework for the Uptake of Oxoâ€Anions from Water. ChemPlusChem, 2021, 86, 699-699.	1.3	1
82	Assembly of two new heterometallic coordination polymers derived from 3-(1 <i>H</i> -benzimidazol-2-yl)propanoic acid. Inorganic and Nano-Metal Chemistry, 2019, 49, 297-305.	0.9	0
83	Degradation pathways of penthiopyrad by l´-MnO <sub>2</sub> mediated processes: a combined density functional theory and experimental study. Environmental Sciences: Processes and Impacts, 2021, 23, 1977-1985.	1.7	0